Spectrophotometric characterization of high proper motion sources from *WISE*

J. C. Beamín,[1,2,3]★ V. D. Ivanov,[1,4] D. Minniti,[3,5,6] R. L. Smart,[7] K. Mužić,[1]
R. A. Mendez,[1,3,8] Y. Beletsky,[9] A. Bayo,[3,10] M. Gromadzki[3,10] and R. Kurtev[3,10]

[1]*European Southern Observatory, Ave. Alonso de Cordoba 3107, Casilla 19001, Santiago, Chile*

[2]*Facultad de Física, Instituto de Astrofísica, Pontificia Universidad Católica de Chile, Casilla 306, Santiago 22, Chile*

[3]*Millennium Institute of Astrophysics, 7500011, Santiago, Chile*

[4]*European Southern Observatory, Karl-Schwarzschild-Str. 2, D-85748 Garching bei München, Germany*

[5]*Facultad de Ciencias Exactas, Universidad Andres Bello, Fernandez Concha 700, Las Condes, Santiago, Chile*

[6]*Vatican Observatory, I-00120 Vatican City State, Italy*

[7]*INAF-Osservatorio Astrofisico di Torino, Strada Osservatorio 20, I-10025 Pino Torinese, TO, Italy*

[8]*Departamento de Astronomía, Universidad de Chile, Camino el Observatorio 1515, Casilla 36-D, Santiago, Chile*

[9]*Las Campanas Observatory, Carnegie Institution of Washington, Colina el Pino, 601 Casilla, La Serena, Chile*

[10]*Instituto de Física y Astronomía, Facultad de Ciencias, Universidad de Valparaíso, Ave. Gran Bretaña 1111, Playa Ancha, Casilla 53, 2340000, Valparaíso, Chile*

ABSTRACT

The census of the solar neighbourhood is almost complete for stars and becoming more complete in the brown dwarf regime. Spectroscopic, photometric and kinematic characterization of nearby objects helps us to understand the local mass function, the binary fraction, and provides new targets for sensitive planet searches. We aim to derive spectral types and spectrophotometric distances of a sample of new high proper motion sources found with the *WISE* (*Wide-field Infrared Survey Explorer*) satellite, and obtain parallaxes for those objects that fall within the area observed by the Vista Variables in the Vía Láctea survey (VVV). We used low-resolution spectroscopy and template fitting to derive spectral types, multiwavelength photometry to characterize the companion candidates and obtain photometric distances. Multi-epoch imaging from the VVV survey was used to measure the parallaxes and proper motions for three sources. We confirm a new T2 brown dwarf within ∼15 pc. We derived optical spectral types for 24 sources, mostly M dwarfs within 50 pc. We addressed the wide binary nature of 16 objects found by the *WISE* mission and previously known high proper motion sources. Six of these are probably members of wide binaries, two of those are new, and present evidence against the physical binary nature of two candidate binary stars found in the literature, and eight that we selected as possible binary systems. We discuss a likely microlensing event produced by a nearby low-mass star and a galaxy, that is to occur in the following five years.

Key words: techniques: spectroscopic – astrometry – parallaxes – brown dwarfs – stars: low-mass.

1 INTRODUCTION

High proper motion (PM) sources have been studied for over two centuries now, as one might expect that the fastest moving sources would be the closest to our Solar system. Since mid 20th century, comprehensive searches of high PM objects have been performed using photographic plates and later CCD cameras to find the closest neighbours of the Sun (Giclas, Burnham & Thomas 1971; Luyten

1979a,b; Wroblewski & Torres 1989; Hambly et al. 2004; Lépine & Shara 2005; Lépine 2008; Finch et al. 2014, Research Consortium on Nearby Stars, among others). However, cool objects are intrinsically faint in the optical and emit most of their light in the near-infrared (NIR). Therefore, the searches for unknown nearby sources gradually turn to the NIR wavelengths taking advantage of improved camera sensitivities, spatial and temporal resolution (Deacon et al. 2009; Kirkpatrick et al. 2010; Smith et al. 2014), yielding in the last 20 yr the discovery of over 2000 ultracool dwarfs. Widening the colour space of the searches has helped to improve the stellar and sub-stellar density estimates in the solar neighbourhood, and the

★ E-mail: jcbeamin@astro.puc.cl

frequency of low-mass companions, among other questions (Allen et al. 2012; Dieterich et al. 2012; Luhman et al. 2012; Ivanov et al. 2013; Deacon et al. 2014; Davison et al. 2015).

The *Wide-field Infrared Survey Explorer* (*WISE*; Wright et al. 2010) satellite has revolutionized the field of brown dwarf with colour-based selections providing the discovery of hundreds of brown dwarfs (Kirkpatrick et al. 2011). Later, the multi-epoch nature of the *WISE* mission provided PMs for over 20 000 individual sources (Kirkpatrick et al. 2014; Luhman 2014a), including the discoveries of the third and the fourth closest systems to the Sun (Luhman 2013, 2014b). These are the closest binary BD, and the coldest BD known. The *WISE* mission also lead to the discovery of the first Y dwarfs (Cushing et al. 2011; Kirkpatrick et al. 2012). Thousands of other interesting objects were found, including young very low mass objects (M, L and T type; Gagné et al. 2015), several ultra-cool sub-dwarfs (Kirkpatrick et al. 2014), etc. These discoveries are helping to better understand the role of temperature, metallicity and evolution in very cool atmospheres. Finally, a new sample of nearby K and M dwarfs ($d \leq 100$ pc) was created, well suited for exoplanet searches.

Here, we report a follow-up study of bright high PM objects detected by Luhman (2014a) and Kirkpatrick et al. (2014), concentrating on objects within 50 pc, wide comoving binaries, and possible members of nearby young moving groups. The project summarized here was motivated by the recent discoveries of nearby stellar and sub-stellar objects (e.g. Artigau et al. 2010; Lucas et al. 2010; Luhman 2013; Mamajek et al. 2013; Scholz 2014, among others), the implications that these findings may have on the stellar census in the Solar neighbourhood (Henry et al. 2006; Faherty et al. 2009; Winters et al. 2015), new results in the multiplicity of young low-mass stars and brown dwarfs in the field and young moving groups (Delorme et al. 2012; Elliott et al. 2014), and even the dynamic interactions of the Solar system (Ivanov et al. 2015; Mamajek et al. 2015). The paper is organized as follows: Section 2 describes the catalogues and methods we used to generate a list of objects of interest, and the instruments we used to follow up and characterize them. In Section 3, the methods for classification are presented. Section 4 describes the distance measurements and comparison of photometric and spectroscopic results. Finally, in Section 5, we discuss individual sources, and present our conclusions in Section 6.

2 SAMPLE SELECTION AND OBSERVATIONS

We started by analysing bright sources in the new catalogues of high PM sources by Luhman (2014a) and Kirkpatrick et al. (2014). We selected the brightest sources with the highest PM that were visible in April from the southern skies (i.e. Dec. < 30), with no previous derived spectral types and no data in the ESO archive. We also performed a cross check with previously known high PM sources from SIMBAD (Wenger et al. 2000). If SIMBAD returned a source within 15 arcmin showing a similar PM, we selected the brighter one between the SIMBAD match and the *WISE* object for spectroscopic followup. We used a relaxed criterion to select candidate companions, i.e. a source with PM ≥ 200 mas yr^{-1} and a position angle of PM within ~30°. These relaxed constraints caused the selection of some spurious pairs, and we discuss this issue in the coming sections. We also created a reduced PM diagram in order to find brown dwarf candidates.

To derive the spectral types of the selected objects, we obtained spectra in the optical and in the NIR for WISE J21210032-6239194 (hereafter WISE 2121-6239). In addition, for the objects located

Table 1. Sample of *WISE* high PM objects selected for spectroscopic follow-up with the EFOSC2 at the NTT at La Silla observatory, and FIRE at Baade at Las Campanas observatory.

Name	RA	Dec.	Exposures
2MASS J06571510−1446173	06:57:14.44	−14:46:25.2	2×120
2MASS J07523088−4709470	07:52:31.93	−47:09:49.8	3×60
2MASS J08291581−5850305	08:29:15.28	−58:50:35.2	2×60
2MASS J09432908−0237184	09:43:28.09	−02:37:22.4	3×60
2MASS J10570299−5103351	10:57:01.20	−51:03:37.2	2×120
2MASS J11161471−4403252	11:16:14.91	−44:03:28.4	2×120
2MASS J11163668−4407495	11:16:36.94	−44:07:47.2	3×120
2MASS J13211484−3629180	13:21:13.94	−36:29:11.1	6×120
2MASS J13552455−1843080	13:55:23.50	−18:43:18.1	5×180
2MASS J14033647+0412395	14:03:36.06	+04:12:28.9	5×180
2MASS J14040025−5923551	14:04:00.52	−59:23:53.3	2×120
2MASS J12412819−6507578	12:41:28.10	−65:07:55.6	2×120
2MASS J13322604−6621419	13:32:26.19	−66:21:33.8	3×120
2MASS J14035016−5923426	14:03:50.92	−59:23:45.2	2×120
2MASS J14233830+0138520	14:23:38.27	+01:38:41.7	3×120
2MASS J14574906−3904511	14:57:49.68	−39:04:55.1	5×180
2MASS J15463089−5258367	15:46:31.10	−52:58:32.1	3×60
2MASS J15480441−5810533	15:48:03.58	−58:10:49.9	2×120
2MASS J17345391−6206546	17:34:53.20	−62:06:52.1	3×15
2MASS J19104599−4133407	19:10:45.27	−41:33:46.9	3×120
2MASS J19242108−0804516	19:24:21.09	−08:04:51.6	2×120
2MASS J20044356−7123334	20:04:43.09	−71:23:28.4	2×120
2MASS J21252081−3422144	21:25:20.78	−34:22:20.3	2×120
2MASS J22275385−2337300	22:27:52.75	−23:37:35.1	3×120
WISE J212100.87−623921.6	21:21:00.88	−62:39:21.7	6×63.4

within the area covered by the VISTA Variables in the Vía Láctea survey (VVV) we obtained photometry and astrometry.

2.1 New Technology Telescope/The ESO Faint Object Spectrograph and Camera v.2

The ESO Faint Object Spectrograph and Camera v.2 (EFOSC2; Buzzoni et al. 1984; Snodgrass et al. 2008) mounted at the 3.6-m New Technology Telescope (NTT) at la Silla observatory, is a versatile instrument for low-resolution spectroscopy, imaging and polarimetry. We obtained low-resolution long-slit spectra for 24 sources (see Table 1) using the same configuration for all the sources: 1 arcsec slit width, grism number one, covering a spectral range of $\lambda = 3185$–10 940 Å[1] with a resolution ~48 Å. All the sources were observed on 2014 April 17. The usual reduction steps, bias and flat-fields corrections were performed, followed by wavelength calibration and flux calibration with the F-type spectrophotometric standard LTT 9239 (Hamuy et al. 1994).

2.2 Magellan/FIRE

The Folded-port Infrared Echellette (FIRE; Simcoe et al. 2008, 2010, 2013) mounted at the 6.5-m Magellan Baade Telescope uses a 2048 × 2048 HAWAII-2RG array. It covers the wavelength range from 0.8 to 2.5 μm when used in the high-throughput prism mode, delivering a resolution varying from ~ 500 the at *J* band to ~300 at the *K* band for the 0.6 arcsec slit. A spectrum of the objects WISE 2121-6239 was obtained in the ABBAAB pattern, with the exposure time of 6 × 63.4 s. The 1 arcsec slit was oriented along the parallactic

---

[1] According to instrument manual, there is second-order contamination for wavelengths longer than 9280 Å.

angle. The read-out mode was 'sample-up-the-ramp' (SUTR) with the low gain mode ($3.8e^-$ per count). The A0V star HD 195288 was observed with the same setup (with the exception of the read-out mode, we used mode 'Fowler 1' instead) in ABBA pattern, for telluric correction. Low- and high-voltage (1.5 and 2.5 V) flats were obtained after the observations of the source and the telluric lines to correct the red and blue parts of the spectrum. NeAr lamp spectra were obtained after the observations for wavelength calibration. In addition, we observed an extra lamp with the 0.45 arcsec slit to differentiate some blends with lines that help us to improve the wavelength calibration.

The data was reduced with the instrument pipeline *firehose_ld*.[2] It traces the slit, performs a wavelength solution, combines the flat-fields and applies them, finding the object on the 2D image, and finally it extracts a 1D spectrum.

The individual spectra of the target and the telluric are median scaled with the *fire_xcombspec* tool and then combined with a robust weighted mean algorithm. Finally, the telluric correction was applied using the *fire_xtellcor_ld*, a clone of the XTELLCOR program from SPEXTOOL (Vacca, Cushing & Rayner 2003; Cushing, Vacca & Rayner 2004).

2.3 Visual and Infrared Survey Telescope for Astronomy/VIRCAM

The VVV survey (Minniti et al. 2010; Saito et al. 2012; Hempel et al. 2014) is one of the six ESO public surveys carried out with the 4.1-m Visual and Infrared Survey Telescope for Astronomy (VISTA) telescope and VIRCAM camera at cerro Paranal Chile (Dalton et al. 2006; Emerson & Sutherland 2010). It has 16 2048 × 2048 pixels chips with a pixel scale of 0.34 arcsec. The total field of view is ~ 1° × 1.5°. The VVV is a variability survey primarily designed to trace the 3D structure of the Milky Way, observing 562 deg² towards the Galactic bulge and southern inner disc (Gonzalez et al. 2011; Dékány et al. 2013; Minniti et al. 2014). This survey matches the requirements for good estimations of the PMs and parallaxes, as demonstrated previously by Beamín et al. (2013) and Ivanov et al. (2013). The data were reduced at the Cambridge Astronomy Survey Unit (CASU) with pipeline v1.3. In this paper, we used the astrometric and photometric catalogues generated from individual exposures (named pawprint, see Hempel et al. 2014 for further details), as opposed to catalogues generated from the combined exposures. This way, we have two independent astrometric/photometric points obtained within a few minutes, where the target is observed by a different detector, giving us a better handling of the systematic uncertainties. We took advantage of the high stellar density of the fields and constructed a local astrometric solution to fit relative PM and parallax simultaneously.

3 SPECTROPHOTOMETRIC CHARACTERIZATION

3.1 Spectral typing

21 of the 24 spectra observed with EFOSC2 showed the characteristic molecular absorption bands M-type stars (TiO, CaH), and they were compared to the primary K5V–M9V standards from Kirkpatrick, Henry & McCarthy (1991) and Kirkpatrick et al. (1999)

available from the Dwarf Archives.[3] The remaining three spectra indicated hotter stars, and for those earlier than K5-type objects we used the standards of Pickles (1998).

The low-resolution of our spectra (~40 Å) does not allow us to use the spectral indexes frequently used in the literature (e.g. Kirkpatrick et al. 1991; Gizis 1997; Lépine et al. 2013) so we relied instead on the overall shape of the spectrum.

The template spectra were smoothed to the resolution of our data, normalized at 7500 Å. To find the best match, we performed a χ^2 minimization over two different wavelength ranges. First for the 20 later type stars, we used the range $\lambda = 6500$–9000 Å, as most of the flux and spectral features of interest are in that region, also the templates from Kirkpatrick et al. (1991) that we used do not cover bluer wavelengths. For the four hotter objects, we minimize over a broader wavelength region, $\lambda = 3500$–9500 Å as they have more flux towards the bluer regions.

The results are shown in Figs 1 and 2. The types of some objects were adjusted by upto 0.5 sub-type after a visual inspection.

The derived spectral types are listed in Table 3. We also attempted to fit separately the blue (6500–7600 Å) and red (7600–9000 Å) parts of each spectrum as shown in Jao et al. (2008) the red part of M sub-dwarfs appears ~1 sub-type earlier than their blue part (depending on metallicity). We did not observe this behaviour in the previously reported sub-dwarf object 2MASS J14574906-3904511.

The NIR spectra of WISE J2121-6239 was compared to the L and T dwarf spectra from the SPEX library[4] using the χ^2 minimization algorithm, mentioned before, yielding a best match to the T2 type SDSS J175024.01+422237.8. Fig. 3 shows the comparison of WISE 2121-6239 against three T sub-types, T1 SDSS J085834.42+325627.7; T2 SDSS J175024.01+422237.8; T3 2MASS J12095613-1004008.

The spectral indexes: H_2O-J, $CH_4 - J$, H_2O-H, $CH_4 - H$ and $CH_4 - K$ from Burgasser et al. (2006) yield a spectral type of T2±1 (Table 2). Using the tabulated coefficients of table 14 in Dupuy & Liu (2012) and the 2MASS and *WISE* magnitudes we computed a photometric distance between 12 and 16 pc for this brown dwarf.

3.2 SED fitting

We searched various archives for historic multiwavelength observations of our programme targets. Using ALADIN (Bonnarel et al. 2000), we were able to retrieve the catalogues and the archival images, for visual inspection to ensure that our high PM target cross identifications were correct. We also used TOPCAT (Taylor 2005) to cross-match catalogues.

To build the SED and compare to stellar models we used the Virtual Observatory SED analyzer (VOSA; Bayo et al. 2008), fitting the BT-settl models 2012 (Allard, Homeier & Freytag 2012) to the data, first with a Bayesian approach, and then constraining the model parameters with a χ^2 minimization over a three parameter space: effective temperature T_{eff}, surface gravity log$g$ and metallicity [Fe/H]. Increasing the number of photometric measurements and widening the wavelength coverage makes the fit more robust and reliable.

The T_{eff} is the most stringently constrained parameter, with uncertainties of order of ~ 200 K. The other parameters log$g$ and [Fe/H], were not well constrained and usually presented flat probabilities distribution in the Bayes analysis. Nevertheless, all the

---
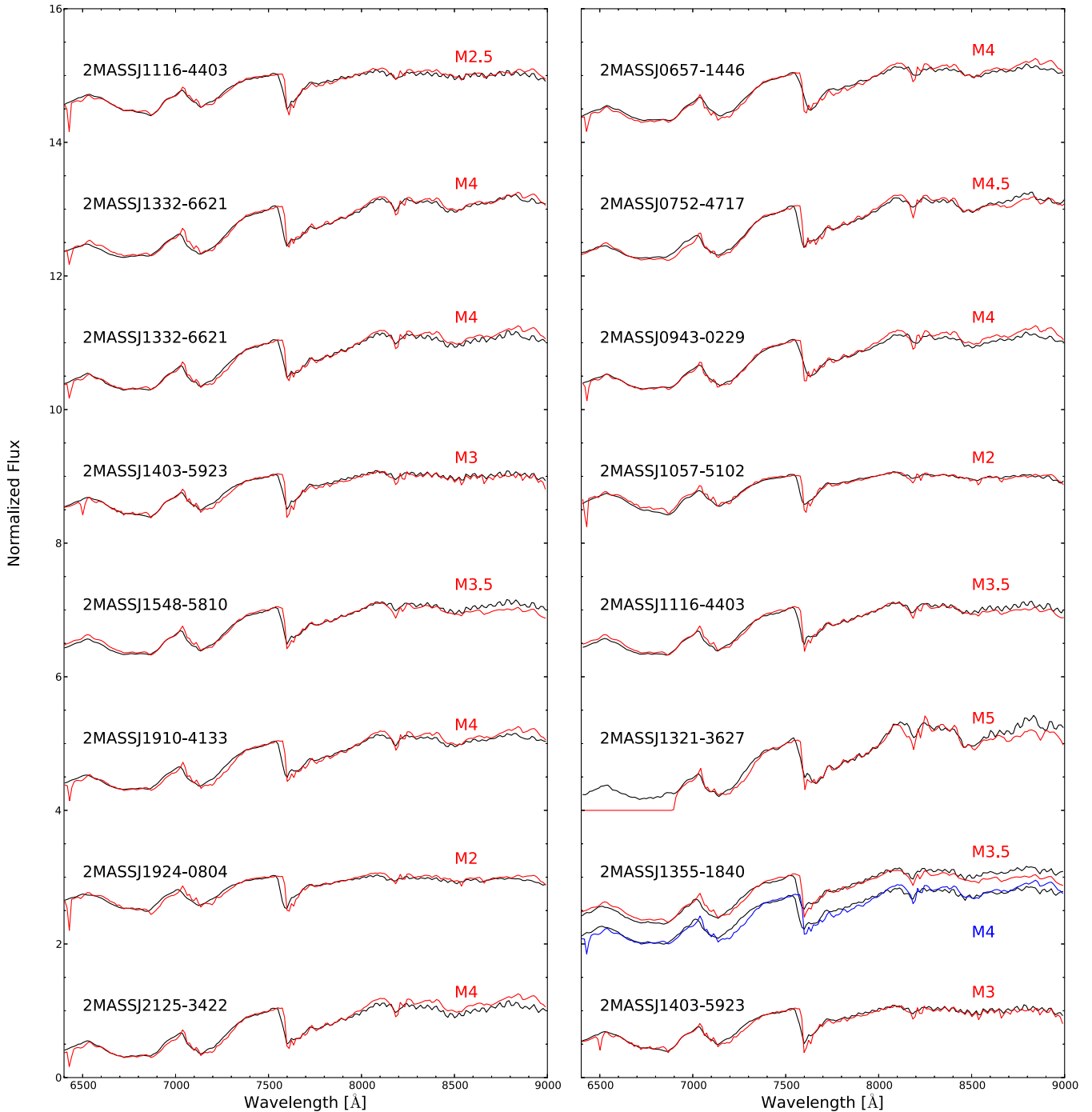
[2] http://web.mit.edu/rsimcoe/www/FIRE/ob_data.htm

[3] http://dwarfarchives.org

[4] http://pono.ucsd.edu/~adam/browndwarfs/spexprism/library.html

Figure 1. Each panel show the best χ^2 fit to the spectrum from the set of spectral templates given in Table 4, the templates spectra are taken from the primary standards from Kirkpatrick et al. (1991). In the case of 2MASS 1355-1840 we overplotted the two best fits, as they fit slightly better different wavelength regions.

sources were fitted with $\log g \geq 4$, and [Fe/H] ≥ -1, the only exception was 2MASS J15463089-5258367, which was better fitted with lower metallicity values ($-2 \leq$ [Fe/H] ≤ -1.5). The photometry used in the SED fit is available in the online version of Table 3.

In order to use the optical catalogues GSC2.3, USNO-B1,UCAC4 and CMC15 (Monet et al. 2003; Lasker et al. 2008; Zacharias et al. 2013; Muiños & Evans 2014), we had to make the following as-

sumptions. The first and second blue/red photographic band from GSC2.3 were used as Johnson *B/R* bands (when two epochs were available for a given band we use the mean). For USNO-B1 we used B_j as Johnson *B* band and V mag as Johnson *V*. For UCAC4 catalogue, when the source had only *R*-band measurement, we used the UCAC *R* filter from vosa, but, in the last release of UCAC4, they do not list the *R* magnitude, they transformed the old optical magnitudes to Johnson *B* and *V* and to Sloan *r*, *i* filters, and we
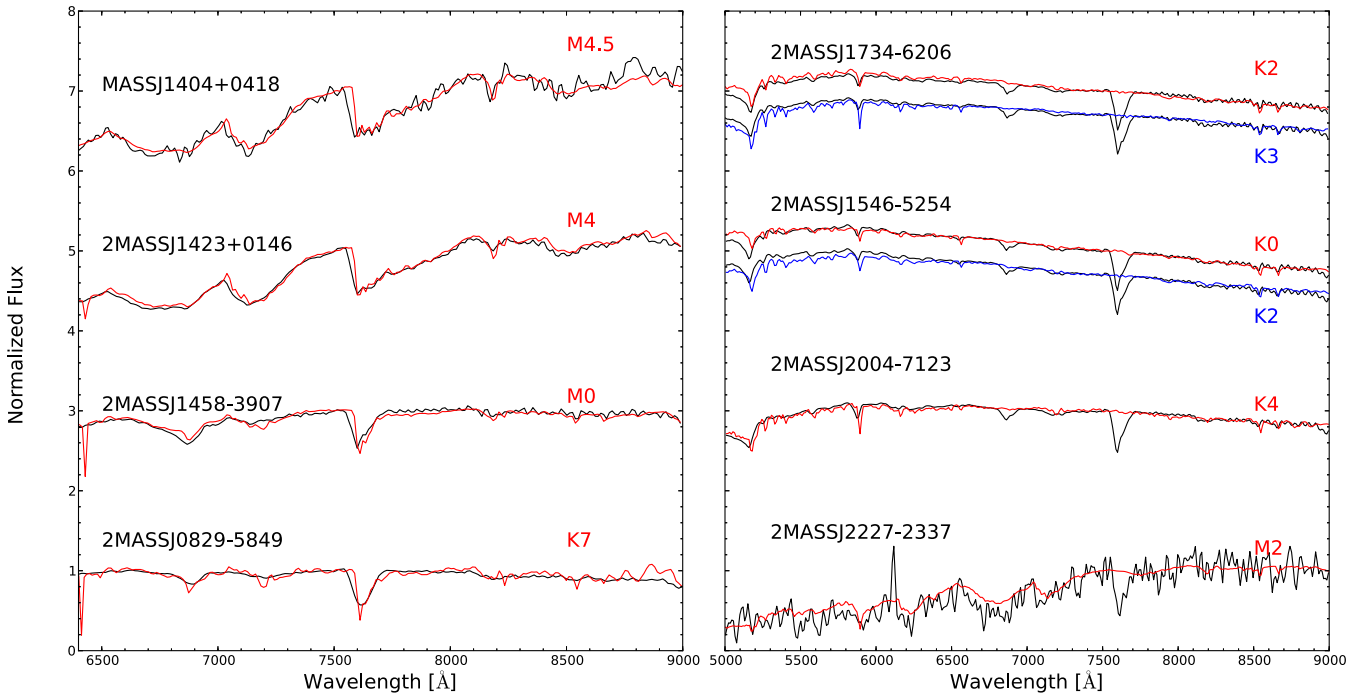
Figure 2. Left-hand panel same as Fig 1. Right-hand panel show the earlier type objects, as the Kirkpatrick et al. (1991) only goes until K5 we used templates from Pickles (1998). For object 2MASS 1546-5252 we assume a K1 spectral type, a compromise between the fit to the continuum of a K0 standard and the Mg absorption around 5170 Å of the K2 standard.
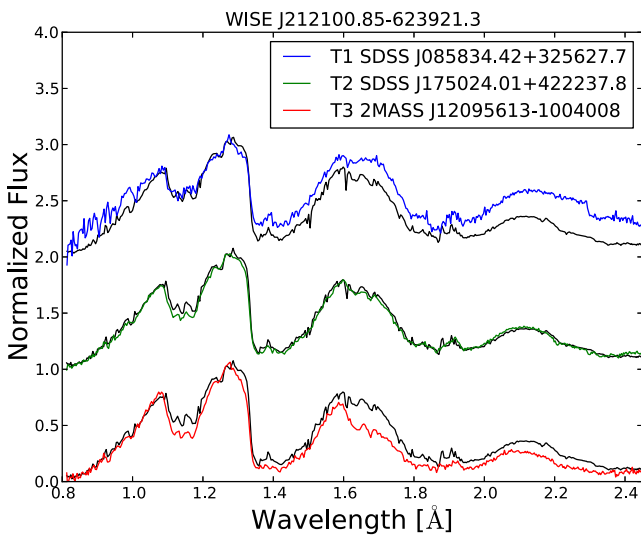

Figure 3. Black spectrum shows the new T2 dwarf WISE 2121-6239 compared to T1 template Burgasser et al. (2010) T2 and T3 template Burgasser et al. (2004).

adopted those values and filter systems. For these three catalogues, we assigned a photometric error of 0.3 mag. CMC15 uses the SDSS *r* filter, the difference with the Sloan *r* system is of the order of 0.02 mag, and a typical error of 0.08 mag at magnitude $r \sim 16$ is listed in the documentation file.[5] To be safe we assumed a fixed value of 0.1 mag for the error in the photometry.

[5] http://svo2.cab.inta-csic.es/vocats/cmc15/docs/CMC15_Documentation.pdf

We performed several simulations letting the uncertainties of USNO-B1, GSC2.3 and UCAC4, vary between 0.2 and 0.5 mag, and removing some of the photometric points to see how much do these assumptions affect the final fit. The SED parameter change within the uncertainties listed above $\Delta T_{\rm eff} \sim 100$ K, $\Delta \log g \sim 0.5$, $\Delta \log g \sim 0.5$.

In Table 4, we provide the object 2MASS name, spectral type from our EFOSC2 spectra and the uncertainty, and the effective temperatures obtained through SED fit using VOSA and archival photometry, using the BT-Settl models (log *g* and metallicities were free parameters and were almost always above 4.5 and −1, respectively).[6]

To compare the spectral and the SED results, we converted the spectral types into effective temperatures using the relations of Pecaut & Mamajek (2013).[7] We found a typical agreement within $\sim$100 K between the two methods.

4 DISTANCE ESTIMATION

4.1 Spectrophotometric distances

We estimated the distances to the objects and their companions from the derived spectral types and $T_{\rm eff}$ from the 2MASS *J* and K_S photometry using the absolute magnitudes from Pecaut & Mamajek (2013). For each object, we calculated the distances for the two bands separately. The mean difference is 3.1 ± 1.7 per cent, with a

[6] The only two objects that were automatically fitted by lower metallicities, 2MASS J1457-3904 and 2MASS J15463089-5258367, are a known subdwarf and an early K star.

[7] We used the table version 2014.09.29, available at http://www.pas.rochester.edu/~emamajek/EEM_dwarf_UBVIJHK_colors_Teff.txt.

Table 2. Main spectral indexes for T dwarfs as given in Burgasser et al. (2006).

Object	H$_2$O-J	CH$_4$-J	H$_2$O-H	CH$_4$-H	CH$_4$-K	Adopted type
WISE J2121-6239	0.55(T2)	0.72(T1)	0.48(T2)	0.93(T1)	0.62(T2)	T2 $\pm$ 1

maximum value of 5.6 per cent for object 2MASS J1403+0412. Our final estimate was the average of the two measurements. The subtype error classification affects the distance estimation by a factor of 15 per cent, on average. The photometric uncertainties introduce errors within 1–3 per cent in the magnitude range we examine. Therefore, estimated spectrophotometric distances will have an associated error of $\lesssim$20 per cent, of the same order as the differences between our measurements and the values available in the literature (Table 4). A comparison between the values for the distances in the literature and the values we obtain in this study is shown in Fig. 4. The error bars correspond to 15 per cent of their distances in each axis. The only exception is 2MASS J1546-5258, as this source has three distances estimates in the literature. We plotted the average value of the distance and quote the standard deviation around the mean as the error.

4.2 Parallax distances

Four objects in our list lie within the VVV survey footprint: 2MASS J14035016-5923426, 2MASS J14040025-5923551, 2MASS J15464497-5254371, 2MASS J15463089-5258367, but the last one is badly saturated in K_S, and reliable positions could not be determined. Therefore, we measure the parallaxes only for the first three sources using the procedure developed in the Torino Observatory Parallax Program described in Smart et al. (2003). This has been adapted to the format of the VVV data products (coordinates and photometry) delivered by CASU.[8] A detailed description of the parallax code can be found in that paper, and we give here only a brief description of the steps involved. For the purpose of the astrometric reduction, we selected reference stars in a circle of radius 1 arcmin around the target which, given the high stellar density in these fields, provides an adequate number of reference stars (above a hundred sources). These were selected among the highest S/N objects in the field of view, satisfying the condition that they appear in at least 80 per cent of the frames, and do not exhibit large PMs.

For example, for 2MASS 15464497-5254371 the initial number of reference stars was 189, but in the end only 121 of these were used to build the astrometric reference frame. In total, we had 70 VVV images in K_S, at various epochs (see Fig. 5), spanning more than 3 yr. Four epochs were excluded from the solution due to their high residuals with respect to the mean solution. Despite the relatively small parallax, the long baseline and the parallax factor coverage provide a small final error of 1.80 mas. The conversion from relative to absolute parallax, which in any case is quite small (less than 0.4 mas), was computed using the Galactic model by Mendez & van Altena (1996), extended to IR wavelengths. The PM and parallaxes for these three sources are listed in Table 4, and Fig. 5 show the observations of each source and the best fits.

The binary system 2MASS J14035016-5923426 and 2MASS J14040025-5923551 was on the border of two adjacent chips in the observational sequence and both objects are very bright often saturating in good seeing. This led to high centroiding errors and a

sparse reference star set of only 41 and 55 objects for the two fields, respectively. The two parallax solutions were therefore completely independent with different reference fields and with observations from different VIRCAM chips.

Each observation has a quote positional error from the VISTA pipeline but there is a significant fraction of the total that is systematic in nature from transforming the observations to a common system. For this reason when calculating the errors of the derived parallax we do not use the individual observation errors. The final quote errors on the target parameters are obtained from the covariance matrix of the solution scaled by the error of unit weight.

The observations used in the sequence are selected using the standard outlier rejection criteria developed in the Torino program following these two criteria: (1) the average per coordinate error of the reference stars in a frame must be less than the mean error of all frames plus three standard deviations about the mean; (2) the combined observed-minus-computed coordinate residual of each observation must be less than three times the sigma of the whole solution. The objects 2MASS J15464497-5254371, 2MASS J14035016-5923426 and 2MASS J14040025-5923551 had 4, 2 and 2 observations rejected respectively by these criteria.

Extensive bootstrap-like testing was carried out on the observations to make sure the results were robust. This consisted of iterating through each observation and using as the primary base frame and thus making a solution that that incorporated slightly different sets of reference stars and a different starting point within the sequence. The solution chosen for publication is that one which is closest to the median of all solutions. The majority of the solutions ($>$90 per cent) were all within one sigma of the chosen solution.

5 DISCUSSION AND REMARKS ON INDIVIDUAL OBJECTS

We determined physical properties and distances for 25 stars, most of which are within $D \sim 140$ pc from the Sun. Only eight of these had previously determined distances. 13 of the stars are located within $D \sim 50$ pc. Given that our selection of targets from the *WISE* high PM list was not systematic, and that the list itself is not a complete census of the objects within $D \sim 50$ pc we did not attempt to do a completeness analysis. The derived spectral types range from early-K to mid-M.

The high transverse velocities of 2MASS J173453.91-620654.6, 2MASS J140336.47+041239.5 and 2MASS J145749.06-390451.1 and the comoving binary pair 2MASS J08291581-5850305 (or L 186-122) and 2MASS J08292286-5849209, make them likely members of the Galactic halo. The remaining objects probably belong to the disc population.

5.1 Probable multiple systems

We adopted binarity criteria requiring: common PMs i.e. $\Delta\theta\Delta\mu \leq (\mu/0.15)^{3.8}$, where $\Delta\theta$ and $\Delta\mu$ are the angular separation (in arcsec) and the difference in the magnitude of the PM vectors (in arcsec yr^{-1}; see section 2.2. in Lépine & Bongiorno 2007), distances in

---

[8] http://casu.ast.cam.ac.uk/surveys-projects/vista/data-processing

Table 3. Archival photometry for sources selected for EFOSC2 spectroscopy and candidate companions.

Column name	Description
2MASS	Name from 2MASS point source catalogue
Spectra	Spectroscopy available for this object
B	B from GSC2.3 or USNO-B1
V	V from GSC2.3 or USNO-B1
R	R from GSC2.3 or USNO-B1
I	I from Super Cosmos I_{IVN}
R_{UCAC}	old R from UCAC4
J_{2MASS}	2MASS J
e_J_{2MASS}	Error in J_{2MASS}
H_{2MASS}	2MASS H
e_H_{2MASS}	Error in H_{2MASS}
K_{S2MASS}	2MASS K_S
e_K_{S2MASS}	Error in K_{S2MASS}
W1	*WISE* W1
e_W1	Error in W1
W2	*WISE* W2
e_W2	Error in W2
W3	*WISE* W3
e_W4	Error in W3
W4	*WISE* W4
e_W4	Error in W4
I_{DENIS}	DENIS I
e_I_{DENIS}	Error in I_{DENIS}
J_{DENIS}	DENIS I
e_J_{DENIS}	Error in J_{DENIS}
$K_{S_{DENIS}}$	DENIS I
$e\_K_{S_{DENIS}}$	Error in $K_{S_{DENIS}}$
u_{SDSS}	SDSS u
e_u_{SDSS}	Error in u_{SDSS}
g_{SDSS}	SDSS g
e_g_{SDSS}	Error in g_{SDSS}
r_{SDSS}	SDSS r or new UCAC4 r[a] or CMC15 r [b]
e_r_{SDSS}	Error in r_{SDSS}
i_{SDSS}	SDSS i or new UCAC4 i[a]
e_i_{SDSS}	Error in i_{SDSS}
z_{SDSS}	SDSS z
e_z_{SDSS}	Error in z_{SDSS}
Y_{UKIDSS}	UKIDSS Y
e_Y_{UKIDSS}	Error in Y_{UKIDSS}
J_{UKIDSS}	UKIDSS J
e_J_{UKIDSS}	Error in J_{UKIDSS}
H_{UKIDSS}	UKIDSS H
e_H_{UKIDSS}	Error in H_{UKIDSS}
K_{UKIDSS}	UKIDSS K
e_K_{UKIDSS}	Error in K_{UKIDSS}
Z_{VVV}	VVV Z
e_Z_{VVV}	Error in Z_{VVV}
Y_{VVV}	VVV Y
e_Y_{VVV}	Error in Y_{VVV}
J_{VVV}	VVV J
e_J_{VVV}	Error in J_{VVV}
H_{VVV}	VVV H
e_H_{VVV}	Error in H_{VVV}
$K_{S_{VVV}}$	VVV K_S
$e\_K_{S_{VVV}}$	Error in $K_{S_{VVV}}$

Notes. SDSS (DR9), GSC2.3, USNO-B1, UCAC4, CMC15, DENIS, VVV (DR3), 2MASS, *WISE* (Epchtein et al. 1997; Lasker et al. 2008; Skrutskie et al. 2006; Lasker et al. 2008; Wright et al. 2010; Ahn et al. 2012; Zacharias et al. 2013; Hempel et al. 2014).
[a]Magnitudes from UCAC4 transformed to SDSS *r* and *i* filters, we assume a fixed error of 0.3 mag.
[b]Magnitudes from CMC15, the catalogue mentions they use an SDSS *r* filter, we assumed 0.1 errors (see discussion of errors in the text).
This table is available in a machine-readable form in the online journal. Headers and description of the columns are shown here for guidance only.

agreement at the 2σ confidence level, and consistency between the spectral types and the apparent magnitudes.

Based on these criteria we identify six probable multiple system, five previously reported systems, and discovering one new one. The following stars are most likely real gravitationally bound systems:

(i) 2MASS J06571510−1446173 (or LP 721-15) and 2MASS J06571773−1446382;

(ii) 2MASS J08291581−5850305 (or L 186-122) and 2MASS J08292286−5849209;

(iii) 2MASS J14040025−5923551 (or L 197-165) and 2MASSJ14035016−5923426;

(iv) 2MASS J15480325−5811119 (or LHS 3119) and 2MASS J15480441−5810533;

(v) 2MASS 19103460−4133443 (or SIPS1910-4133A), 2MASS 19104599−4133407(or SIPS1910-4133B) and 2MASS 19103359-4132505 (or SIPS1910-4132C);

(vi) 2MASS J20044356−7123334 (or LTT 7914) and 2MASS J20043661−7123532.

Their parameters are listed in Table 5.

The triple system 2MASS 19103460-4133443, 2MASS 19104599-4133407 B and 2MASS 19103359-4132505 C was reported by Lépine (2005), Deacon et al. (2005) and Hambly & Deacon (2005). The last work discussed the possibility that this is actually a quadruple system because the magnitude of the component B is ∼0.5 mag brighter than the C component. The spectrophotometric and SED based distances all agree within the 1σ errors (see Table 5. When we compare the T_{eff} obtained via SED fit of components B and C we find a difference of ∼200 K which would be sufficient to explain the 0.5 mag difference (that difference can be less given the error bars for temperature estimates). But we think that is not necessary to invoke a possible equal mass unresolved binary in component B to explain that difference in magnitude, and it is more likely to be explained as an effect of slight difference (∼100–200 K) in T_{eff}.

2MASS J14040025-5923551 and 2MASSJ14035016-5923426 are comoving. Our spectra suggest this is an M3+M2.5 nearly equal mass binary. Despite the saturation, we were able to measure a parallax from the multi-epoch VVV data: 40.35 ± 7.19 mas and 49.07 ± 7.06 mas ($24.78^{+5.4}_{-3.7}$ pc and $20.4^{+3.4}_{-2.6}$ pc), respectively.

2MASS J20044356-7123334 (or LTT 7914) was observed by the RAdial Velocity Experiment (RAVE) in its fourth data release Kordopatis et al. (2013) and described there. They derived a $T_{eff} = 4817$ and $\log g = 4$ and metallicity [Fe/H] $= 0.05$, based on this we could assume the dwarf nature and apply the relations described before, deriving a distance of 108 pc. They also obtained a radial velocity of $RV_{Heliocentric} = -50.2 \pm 2.2$ km s^{-1} Our best spectral type for this object is K2, the reference T_{eff} for a K2V star is ∼5000 K so our classification might be revised by one sub-type. Applying photometric SED fitting, we obtained a $T_{eff} = 4500$ K ± 100, $\log g = 5 \pm 1$ and metallicity [Fe/H] $= 0.3 \pm 0.5$ The photometric spectral type would be K4, which is two spectral types later than the fit from our optical spectroscopy and one later than the type inferred by RAVE. For a range of photometric distances for K2–K4 types we obtain distances of 100–130 pc, implying a tangential velocity of 170–225 km s^{-1}, typical for thick disc or halo objects. Interestingly, the available data do not support a low metallicity for this object. For the comoving star 2MASS J20043661-7123532 the best photometric fit was $T_{eff} = 3100$ K ± 100, $\log g = 5.5 \pm 1$ and metallicity [Fe/H] $= -1 \pm 0.5$. Assuming a spectral type of M4–M5, the distance would be 80–120 pc in agreement within the errors to the estimated value for 2MASS J20044356-7123334. The

Characterization of high proper motion sources

Table 4. Spectral classification and spectrophotometric distances for the stars observed with EFOSC2@NTT.

2MASS name	Sp. type	SED T_{eff}	J	$\mu_\alpha\cos(\delta)$[mas]	μ_δ[mas]	d[pc] (lit.)	d[pc](this work)	Ref.
J06571510−1446173	M4 ±0.5	3300	10.678	70	−270	–	29.1	This work[a]
J07523088−4709470	M4.5 ±0.5	3200	11.738	−109	176	44.1[b]	38.2	4
J08291581−5850305	K7 ±1	4200	10.206	382	−74	–	80.3	5
J09432908−0237184	M4 ±0.5	3200	10.869	−200	−95	–	31.0	4
J10570299−5103351	M2 ±0.5	3500	11.155	−617	78	54.1	73.0	6
J11161471−4403252	M2.5 ±0.5	3600	10.649	−492	−3	–	52.2	1
J11163668−4407495	M3.5 ±0.5	3300	9.917	−518	−29	21.5[b]	25.6	2
J12412819−6507578	M4 ±0.5	3100	10.526	−499	−081	–	26.2	1
J13211484−3629180	M5 ±0.5	2900	12.136	−513	−209	38.4	37.7	6
J13322604−6621419	M4 ±0.5	3200	10.826	−294	226	–	31.4	1
J13552455−1843080	M4 ±0.5	3200	14.042	−317	−96	–	136.1	3
J14033647+0412395	M4.5 ±1	3000	15.853	−233	−073	–	250.3	7
J14035016−5923426	M3 ±0.5	3500	10.258	11.5 ± 5.1	−492.2 ± 4.3	–	$20.4^{+3.4}_{-2.6}$	This work
J14040025−5923551	M2.5 ±0.5	3600	10.219	8.3 ± 5.9	−494.5 ± 5.1	–	$24.8^{+5.4}_{-3.7}$	This work
J14233830+0138520	M4 ±1	3000	12.374	−221	−195	–	52.8	7
J14574906−3904511	M0 ±1	3900	13.693	−121	−405	215.6	328.6	6
J15463089−5258367	K1 ±1	4700	8.737	−217	−199	44[b];77[b];56[b]	71.3	8,9,10
J15464497−5254371	–	3100	12.340	−296.6 ± 0.8	−109.8 ± 0.9	–	$42.6^{+3.6}_{-3.0}$	This work
J15480441−5810533	M3.5 ±0.5	3400	10.169	−503	−207	33.9[c]	29.5	1,10
J17345391−6206546	K3 ±1	4800	10.364	−203	−390	–	131.5	1
J19104599−4133407	M4 ±0.5	3300	10.610	68	−735	22.8[d]	27.6	2
J19242108−0804516	M2 ±0.5	3700	10.766	−196	−379	–	59.8	1
J20044356−7123334	K4 ±1	4500	10.168	80	−360	–	108.2	3
J21252081−3422144	M4 ±0.5	3300	10.895	− 35	−450	–	32.3	1
J22275385−2337300	M2 ±1	3600	14.422	− 62	−176	–	322.0	3

The photometric distance error from this work are $\lesssim 20$ per cent.

[a]We recalculated the PM using 2MASS and the *WISE* ALL-SKY epoch position with the highest S/N, as we find that the Salim & Gould (2003) value for PM of LP 721-15 is inconsistent with the motion of the sources in the images, this object could be an unresolved binary, and then located furher away, see text for discussion.

[b]Photometric distance (spectral type derived from T_{eff} using the relations in Pecaut & Mamajek (2013) and online table maintained by E. Mamajek, see text for the link).

[c]Parallax distance.

[d]The paper cites the value for other object of the system (SIPS 1910-4133A) and is from photographic plates, our measurement is for SIPS 1910-4133B. The values of PM and distances with quoted errors were fitted from VVV data: (1) Luhman (2014a) ; (2) Winters et al. (2015); (3) Salim & Gould (2003) ; (4) Finch et al. (2007); (5) Luyten & Hughes (1980); (6) Subasavage et al. (2005a); (7) Lépine & Shara (2005); (8) Ammons et al. (2006) (9) Fresneau, Vaughan & Argyle (2007); (10) Pickles & Depagne (2010).
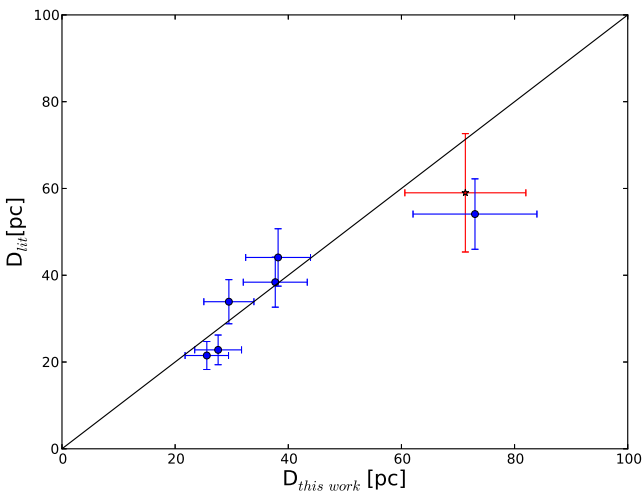

Figure 4. Literature photometric distances versus spectrophotometric distances from this work for objects within 100 pc. The red star represents the average of the three distance from the literature for source 2MASS J1546-5258, and the error in the Y-axis for this source is the dispersion around the mean. The solid black line shows a 1:1 relation, and not a fit to the data points.

objects are separated by 38.7 arcsec on the sky, which corresponds to ~4200 au for a distance of 110 pc.

Object 2MASS J22275385-2337300 (or LP 876-22) was observed by mistake, as the real new binary candidate was LP 876-1 and 2MASS J22274199-2337283. The observed target was classified as M2 ± 1 star, if we compute the distance we obtain 322 pc which will put this object in a tangential velocity over 250 km s^{-1} and hence probably this object belongs to the halo population, but the distance might be considerably less if we consider that this object might be metal poor, as happened to be with previous sources. We perform the SED fitting to the comoving pair LP 876-1, 2MASS J22274199-2337283 and they were classified as an M3.5–M8.5, that would imply a distance between 40–50 pc, but further observations are required to settle their true nature.

5.2 Rejected multiple systems

The following objects are not real physical pairs, the argument for rejecting them as binaries are the total PM, position angle of motion, spectral types compared to photometric spectral type and distances estimates for the primary and secondary, do not agree within the expected errors.
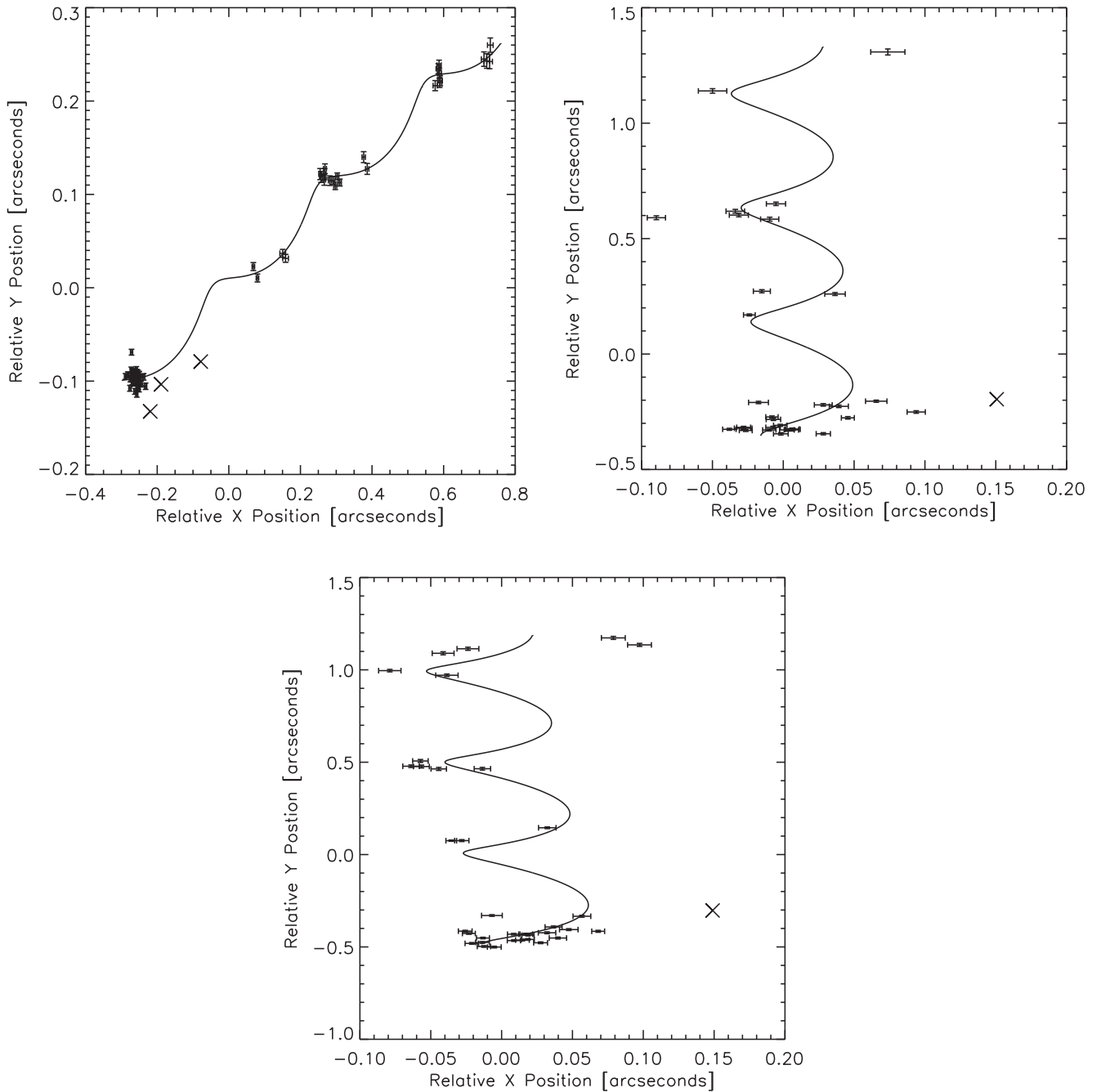
Downloaded from http://mnras.oxfordjournals.org/ at Universidad de Chile on November 13, 2015

MNRAS **454**, 4054–4065 (2015)

Figure 5. Relative displacement of the targets 2MASS 15464497-5254371, 2MASS J14040025-5923551 and 2MASS J14035016-5923426 with respect to the adopted reference frame as a function of time (top of each plot epoch 2010, bottom of each plot, epoch 2013). A base-frame was chosen for the registration of all other frames to account for small offsets and rotation between them. The fitted parallax wobble, shown by the solid line, is clearly seen in the observations which are plotted as crossed error bars representing the formal VISTA pipeline errors. Any rejected observations within the plot ranges are plotted as Xs.

(i) 2MASS J07523088-4709470 and 2MASS J07523777-4717270;

(ii) 2MASS J09432908-0237184 and 2MASS J09434389-0229570;

(iii) 2MASS J10570299-5103351 and 2MASS J10573037-5102190;

(iv) 2MASS J11163668-4407495 (or LHS 2386) and 2MASS J11161471-4403252 (see text);

(v) 2MASS J13211484-3629180 and 2MASS J13214404-3627316;

(vi) 2MASS J13552455-1843080 (or LP 799-1) and 2MASS J13553933-1840586;

(vii) 2MASS J14033647+0412395 and 2MASS J14040651+0418532;

(viii) 2MASS J14233830+0138520 and 2MASS J14234208+0146235;

(ix) 2MASS J14574906-3904511 and 2MASS J14582414-3907504;

(x) 2MASS J15463089-5258367 and 2MASS J15464497-5254371.

Table 5. Binary/multiple system investigated in this paper. The columns are spectral type are from this work and from literature spectra, $T_{\rm eff}$ is defined based on photometric spectral energy distribution, 2MASS J band magnitude, ρ the angular separation in arcsec, D is the photometric distance in pc, except for the labelled objects which have parallaxes, $\mu_\alpha\cos(\delta)$ and μ_δ are the PM in each celestial coordinate.

Star ID	Sp. type (reference)	$T_{\rm eff}$ (K)	$J_{\rm 2MASS}$ (mag)	ρ (arcsec)	Dist. (pc)	$\mu_\alpha\cos(\delta)$ (mas)	μ_δ (mas)	Remarks
2MASS J06571510-1446173	M4	3300	10.678	43.6	29.1	70	−270	See ^{b} in Table 4
2MASS J06571773-1446382	–	3000	12.751	–	∼ 40	61 (1)	−268 (1)	
2MASS J08291581-5850305	K7	4200	10.206	88.49	80.3	363 (4)	−81(4)	Halo wide binary
2MASS J08292286-5849209	–	2900	14.550	–	∼110	355	−73(1)	
2MASS J14040025-5923551	M2.5	3600	10.219	78.05	$24.78^{+5.4}_{-3.7}$	8.27 ± 5.9	$−494.5 \pm 5.1$	VVV parallax
2MASS J14035016-5923426	M3	3500	10.258	–	$20.4^{+3.4}_{-2.6}$	11.5 ± 4.6	$−492.2 \pm 4.3$	
2MASS J15480325-5811119	M1.5(1)	3467(7)	8.379	20.7	23.5(1) 33.6(2)	−593 (1)	−250 (1)	$V_{\rm rad} = 30.9$ km s^{-1} (1)
2MASS J15480441-5810533	M3.5	3400	10.169	–	29.5	−503 (3)	−207 (3)	
2MASS 19103460-4133443	–	3500	9.851	127.78(A−B) 54.99(A−C)	35.9	72 (5)	−738(5)	Triple system
2MASS 19104599-4133407	M4	3300	10.610	147.90(B−C)	22.8 (6) 27.6	91 (5)	−742 (5)	Component B
2MASS 19103359-4132505	–	3100	11.147	–	29.2	68 (5)	−735 (5)	Component C

Notes. (1) Hawley, Gizis & Reid ([1996](#)), (2) van Altena, Lee & Hoffleit ([1995](#)), (3) Luhman ([2014a](#)) (4) Kirkpatrick et al. ([2014](#)), (5) Deacon et al. ([2005](#)), (6) Winters et al. ([2015](#)), (7) Houdebine ([2010](#)). The values without reference were calculated or derived in this work, the photometric distances have a $\lesssim 20$ per cent error (spectral type and effective temperature uncertainties are the main source of error).

2MASS J07523088-4709470 and 2MASS J07523777-4717270: The second object moves ∼2 times faster than the first object ($>5\sigma$ outlier) and the derived $T_{\rm eff}$ of the secondary (the fainter source) is 200 K higher. Given the classification of M4.5V for the primary, this would place the secondary at least twice as far.

2MASS J11163668-4407495 (or LHS 2386) and 2MASS J11161471-4403252 these were classified and found to be a comoving pair observed by G.P. Kuiper and reclassified in Bidelman ([1985](#)), he classified LHS 2386 as M3: We obtain a best fit with M3.5V and M2.5 for 2MASS J11161471-4403252. Luhman & Sheppard ([2014](#)) list these sources as a comoving binary, because the difference in total PM and position angle is small (4.5 and 1.6 per cent, respectively). Also the probability of being a chance alignment is below 10 per cent based on the criteria from Lépine & Bongiorno ([2007](#)). However, the distance we derive for the two stars are only consistent at 3σ level. We obtain half the distance for LHS 2386 than for 2MASS J11161471-4403252. Even if 2MASS J11161471-4403252 is an equal mass binary that would place it around 44–50 pc ∼10–15 pc farther away than we expect for LHS 2386. In this hypothetical case, the distances will agree within the errors, that would mean that at 5.9 arcmin of angular separation and distances between 44 and 50 pc, the projected physical separation would be ∼15 000–20 000 au which would place them as one of the scarce population of very low mass and very wide binaries within 50 pc. Radial velocities of both stars and a more robust estimation of their distances are needed to disentangle their true nature, but we do not list it as a physical pair with the present evidence.

2MASS J14574906-3904511 and 2MASS J14582414-3907504 have PMs that agree within 1 per cent when comparing the 2MASS and *WISE* positions, and the position angle of the motion differ only by 1°, these stars should probably be a real physical pair. On the other hand the inferred spectrophotometric distance for the primary is 328.7 pc, while for the secondary using the SED fit we obtain a distance around 40 pc for spectral type M7. In Jao et al. ([2008](#)) they found that the primary object is actually a MI.0VI sub-dwarf and the distance derived by Subasavage et al. ([2005a](#)) is 215.6 pc even assuming this shorter distance the object is not consistent

with a real binary and would imply a high tangential velocity of 432 km s^{-1}. Finally, the angular separation of 445.9 arcsec means that the projected physical separation at 215.6 pc would be 0.466 pc. Combining these two arguments we argue this is not a real binary.

2MASS J15463089-5258367 and 2MASS J15464497-5254371 Ammons et al. ([2006](#)) derived a distance 44^{+30}_{-15} pc and estimated a $T_{\rm eff} = 4669$–4754 K (according to different fitting functions) based on *Hipparcos* (Tycho) data for the first object. Other two attempts to measure the distance from photometry are available from Fresneau et al. ([2007](#)) and Pickles & Depagne ([2010](#)) they obtained 56 pc (no error bars) and 77^{+50}_{-22} pc, respectively. Our best SED fit yields 4700 K, in agreement with Ammons et al. ([2006](#)), but our best spectrum fit is between K0V and K2V. If we assume this as the correct spectral type, then the photometric distance we obtain is between 68 and 77 pc, for K0–K2 respectively. For the second object, we were able to derive a distance based on parallax from VVV, as discussed in the previous section $\pi = 23.5 \pm 1.8$ mas ($42.6^{+3.6}_{-3.0}$ pc). The parallax and PM of 2MASS J15464497-5254371 are shown in Fig. [5](#) and Table [4](#). The distance agrees very well with the value derived by Ammons et al. ([2006](#)), but is almost 3σ away from the photometric distance to 2MASS J15463089-5258367, in addition to the difference in the PM between the primary (from Tycho-2 catalogue; Høg et al. [2000](#)) and our measurements for the candidate companion are too large. The evidence does not support that these two stars form a real binary, the parallax and more accurate PMs for both sources will be measured by *Gaia* mission, and then the true nature of these objects will be settled.

5.3 Possible future microlensing event

While looking for the available photometry for the object NLTT 37178 from the virtual observatory, we found a nearby source, classified as extragalactic (photometric redshift 0.13) with photometry from SDSS and *GALEX*. In the following years this object will be getting closer until the closest approach to the centre, with the closest approach of 0.6 arcsec in 4–8 yr. Some extended emission in the galaxy is visible on SDSS images, and we can expect that the

nearby star can act as a lens for the outskirts of this galaxy. Deep *U* and *B* band pre-lensing observations are needed to characterize the background source. Search for microlensing events during the next few years may be promising. The most favourable filters to observe the galaxy will be *U*, *B* (and/or UV filters from space). The microlensing event might help to understand the real nature and physical properties of this object, e.g. if it is an unresolved binary or hosts a planet. More robust distance estimations (parallax) are necessary, to better constrain the Einstein radius for the system. We assumed a mass of $0.2M_\odot$ for the lens and distances of 40 pc and 543.9 Mpc(comoving radial distance[9]) for lens and source, respectively, and obtain a crude estimate of the Einstein radius of 6.4 mas. As the lensed source is resolved, we might expect variations on the light curve due to lens magnifying different parts of the galaxy.

6 CONCLUSIONS

We performed spectroscopic follow up for over 20 new high PM objects found by the *WISE* satellite, and looked for possible new wide binary companions. We found one T2 dwarf probably located within 15 pc. We obtained optical spectral types and photometric distances for 24 objects, as well as parallax measurements for three of them. We present some additional evidence for six comoving objects that are likely physical pairs, two of them are new binary candidates. Four objects are probable members of the galactic halo given their large tangential velocities.

Most of the objects analysed in this study are located within 75 pc from the Sun, and are bright enough for further follow-up and search for planets using state of the art and upcoming NIR instruments.

The use of relatively loose constraints when selecting possible wide comoving companions given the inhomogeneity of resources available in the literature prove useful to find new comoving stars. This causes many false positives, but they can be eliminated a posteriori using multiple arguments, combining PM, physical separation and spectral energy distributions in the calculation of photometric distances. It is also important to emphasize the relevance of obtaining distances or spectral types for discriminating chance alignments from real wide binaries (or comoving stars), even when the PM and position probabilities are very low we show two examples in this paper where the hypothesized binaries are most likely not physically related.

We also discussed a likely microlensing event due to a star passing in front of a background galaxy. The number of predicted microlensing events of this type will be more frequent as more HPM low-mass objects are found in high density environments like the galactic bulge and inner disc, but also with background galaxies. Although the lens candidate we present here is not predicted to pass in front of the centre of the galaxy the event can be used to study the lens for unresolved companions and planets. In this case this maybe particularly difficult as the lens goes through different parts of the galaxy in short time-scales magnifying regions of intrinsically different brightness. These events can also be used to make more detailed structural studies of galaxies at low redshift.

ACKNOWLEDGEMENTS

The authors thank the referee Dr. Nigel Hambly for his comments and suggestions that helped to the improve the quality of the pa-

REFERENCES

Ahn C. P. et al., 2012, ApJS, 203, 21

Allard F., Homeier D., Freytag B., 2012, Phil. Trans. R. Soc. A, 370, 2765

Allen P. R., Burgasser A. J., Faherty J. K., Kirkpatrick J. D., 2012, AJ, 144, 62

Ammons S. M., Robinson S. E., Strader J., Laughlin G., Fischer D., Wolf A., 2006, ApJ, 638, 1004

Artigau É., Radigan J., Folkes S., Jayawardhana R., Kurtev R., Lafrenière D., Doyon R., Borissova J., 2010, ApJ, 718, L38

Bayo A., Rodrigo C., Barrado Y Navascués D., Solano E., Gutiérrez R., Morales-Calderón M., Allard F., 2008, A&A, 492, 277

Beamín J. C. et al., 2013, A&A, 557, L8

Bidelman W. P., 1985, ApJS, 59, 197

Bonnarel F. et al., 2000, A&AS, 143, 33

Burgasser A. J., McElwain M. W., Kirkpatrick J. D., Cruz K. L., Tinney C. G., Reid I. N., 2004, AJ, 127, 2856

Burgasser A. J., Geballe T. R., Leggett S. K., Kirkpatrick J. D., Golimowski D. A., 2006, ApJ, 637, 1067

Burgasser A. J., Cruz K. L., Cushing M., Gelino C. R., Looper D. L., Faherty J. K., Kirkpatrick J. D., Reid I. N., 2010, ApJ, 710, 1142

Buzzoni B. et al., 1984, The Messenger, 38, 9

Cushing M. C., Vacca W. D., Rayner J. T., 2004, PASP, 116, 362

Cushing M. C. et al., 2011, ApJ, 743, 50

Dalton G. B. et al., 2006, Proc. SPIE, 6269, 62690X

Davison C. L. et al., 2015, AJ, 149, 106

Deacon N. R., Hambly N. C., Cooke J. A., 2005, A&A, 435, 363

Deacon N. R., Hambly N. C., King R. R., McCaughrean M. J., 2009, MNRAS, 394, 857

Deacon N. R. et al., 2014, ApJ, 792, 119

Dékány I., Minniti D., Catelan M., Zoccali M., Saito R. K., Hempel M., Gonzalez O. A., 2013, ApJ, 776, L19

Delorme P., Lagrange A. M., Chauvin G., Bonavita M., Lacour S., Bonnefoy M., Ehrenreich D., Beust H., 2012, A&A, 539, A72

Dieterich S. B., Henry T. J., Golimowski D. A., Krist J. E., Tanner A. M., 2012, AJ, 144, 64

[9] Value obtained using the NED cosmological calculator http://www.astro.ucla.edu/wright/CosmoCalc.html

Dupuy T. J., Liu M. C., 2012, ApJS, 201, 19
Elliott P., Bayo A., Melo C. H. F., Torres C. A. O., Sterzik M., Quast G. R., 2014, A&A, 568, A26
Emerson J., Sutherland W., 2010, The Messenger, 139, 2
Epchtein N. et al., 1997, The Messenger, 87, 27
Faherty J. K., Burgasser A. J., Cruz K. L., Shara M. M., Walter F. M., Gelino C. R., 2009, AJ, 137, 1
Finch C. T., Henry T. J., Subasavage J. P., Jao W.-C., Hambly N. C., 2007, AJ, 133, 2898
Finch C. T., Zacharias N., Subasavage J. P., Henry T. J., Riedel A. R., 2014, AJ, 148, 119
Fresneau A., Vaughan A. E., Argyle R. W., 2007, A&A, 469, 1221
Gagné J. et al., 2015, ApJS, 219, 33
Giclas H. L., Burnham R., Thomas N. G., 1971, Lowell Proper Motion Survey. Northern Hemisphere. The G Numbered Stars: 8991 Stars Fainter Than Magnitude 8 with Motions >0.″26/year. Lowell Observatory, Arizona
Gizis J. E., 1997, AJ, 113, 806
Gonzalez O. A., Rejkuba M., Minniti D., Zoccali M., Valenti E., Saito R. K., 2011, A&A, 534, LL14
Hambly N. C., Deacon N. R., 2005, Astron. Nachr., 326, 1011
Hambly N. C., Henry T. J., Subasavage J. P., Brown M. A., Jao W.-C., 2004, AJ, 128, 437
Hamuy M., Suntzeff N. B., Heathcote S. R., Walker A. R., Gigoux P., Phillips M. M., 1994, PASP, 106, 566
Hawley S. L., Gizis J. E., Reid I. N., 1996, AJ, 112, 2799
Hempel M. et al., 2014, The Messenger, 155, 29
Henry T. J., Jao W.-C., Subasavage J. P., Beaulieu T. D., Ianna P. A., Costa E., Méndez R. A., 2006, AJ, 132, 2360
Houdebine E. R., 2010, MNRAS, 407, 1657
Høg E. et al., 2000, A&A, 355, L27
Ivanov V. D. et al., 2013, A&A, 560, A21
Ivanov V. D. et al., 2015, A&A, 574, A64
Jao W.-C., Henry T. J., Beaulieu T. D., Subasavage J. P., 2008, AJ, 136, 840
Kirkpatrick J. D., Henry T. J., McCarthy D. W., Jr, 1991, ApJS, 77, 417
Kirkpatrick J. D. et al., 1999, ApJ, 519, 802
Kirkpatrick J. D. et al., 2010, ApJS, 190, 100
Kirkpatrick J. D. et al., 2011, ApJS, 197, 19
Kirkpatrick J. D. et al., 2012, ApJ, 753, 156
Kirkpatrick J. D. et al., 2014, ApJ, 783, 122
Kordopatis G. et al., 2013, AJ, 146, 134
Lasker B. M. et al., 2008, AJ, 136, 735
Lépine S., 2005, AJ, 130, 1247
Lépine S., 2008, AJ, 135, 2177
Lépine S., Bongiorno B., 2007, AJ, 133, 889
Lépine S., Shara M. M., 2005, AJ, 129, 1483
Lépine S., Hilton E. J., Mann A. W., Wilde M., Rojas-Ayala B., Cruz K. L., Gaidos E., 2013, AJ, 145, 102
Lucas P. W. et al., 2010, MNRAS, 408, L56
Luhman K. L., 2013, ApJ, 767, L1
Luhman K. L., 2014a, ApJ, 781, 4
Luhman K. L., 2014b, ApJ, 786, L18
Luhman K. L., Sheppard S. S., 2014, ApJ, 787, 126
Luhman K. L. et al., 2012, ApJ, 760, 152
Luyten W. J., 1979a, New Luyten Catalogue of Stars with Proper Motions Larger Than Two Tenths of an Arcsecond. University of Minnesota, MN, USA
Luyten W. J., 1979b, NLTT catalogue. 2nd ed., University of Minnesota, MN, USA Vol. I, p. 282; Vol. II, p. 286
Luyten W. J., Hughes H. S., 1980, Proper Motion Survey with the Forty-Eight Inch Schmidt Telescope. Univ. Minnesota, MN, USA

Mamajek E. E. et al., 2013, AJ, 146, 154
Mamajek E. E., Barenfeld S. A., Ivanov V. D., Kniazev A. Y., Väisänen P., Beletsky Y., Boffin H. M. J., 2015, ApJ, 800, L17
Mendez R. A., van Altena W. F., 1996, AJ, 112, 655
Minniti D. et al., 2010, New Astron., 15, 433
Minniti D. et al., 2014, A&A, 571, A91
Monet D. G. et al., 2003, AJ, 125, 984
Muiños J. L., Evans D. W., 2014, Astron. Nachr., 335, 367
Pecaut M. J., Mamajek E. E., 2013, ApJS, 208, 9
Pickles A. J., 1998, PASP, 110, 863
Pickles A., Depagne É, 2010, PASP, 122, 1437
Saito R. K. et al., 2012, A&A, 537, A107
Salim S., Gould A., 2003, ApJ, 582, 1011
Scholz R.-D., 2014, A&A, 561, A113
Simcoe R. A. et al., 2008, Proc. SPIE, 7014, 70140U
Simcoe R. A. et al., 2010, Proc. SPIE, 7735, 773514
Simcoe R. A. et al., 2013, PASP, 125, 270
Skrutskie M. F. et al., 2006, AJ, 131, 1163
Smart R. L. et al., 2003, A&A, 404, 317
Smith L., Lucas P. W., Burningham B., Jones H. R. A., Smart R. L., Andrei A. H., Catalán S., Pinfield D. J., 2014, MNRAS, 437, 3603
Snodgrass C., Saviane I., Monaco L., Sinclaire P., 2008, The Messenger, 132, 18
Subasavage J. P., Henry T. J., Hambly N. C., Brown M. A., Jao W.-C., 2005a, AJ, 129, 413
Taylor M. B., 2005, in Shopbell P. L., Britton M. C., Ebert R., eds, ASP Conf. Ser. Vol. 347, Astronomical Data Analysis Software and Systems XIV. Astron. Soc. Pac., San Francisco, p. 29
Vacca W. D., Cushing M. C., Rayner J. T., 2003, PASP, 115, 389
van Altena W. F., Lee J. T., Hoffleit E. D., 1995, The General Catalogue of Trigonometric Stellar Parallaxes: Containing Parallax Data Compiled Through November 1995, 4th edn. Yale Univ. Observatory, New Haven, CT
Wenger M. et al., 2000, A&AS, 143, 9
Winters J. G. et al., 2015, AJ, 149, 5
Wright E. L. et al., 2010, AJ, 140, 1868
Wroblewski H., Torres C., 1989, A&AS, 78, 231
Zacharias N., Finch C. T., Girard T. M., Henden A., Bartlett J. L., Monet D. G., Zacharias M. I., 2013, AJ, 145, 44

SUPPORTING INFORMATION

Additional Supporting Information may be found in the online version of this article:

Table 3. Archival photometry for sources selected for EFOSC2 spectroscopy and candidate companions (http://www.mnras.oxfordjournals.org/lookup/suppl/doi:10.1093/mnras/stv2241/-/DC1).

Please note: Oxford University Press is not responsible for the content or functionality of any supporting materials supplied by the authors. Any queries (other than missing material) should be directed to the corresponding author for the article.

This paper has been typeset from a TEX/LATEX file prepared by the author.